Biomechanics and Modeling in Mechanobiology (2018) 17:1599–1610
https://doi.org/10.1007/s10237-018-1046-3

ORIGINAL PAPER

Thermal analysis of the dentine tubule under hot and cold stimuli using fluid–structure interaction simulation

Seifollah Gholampour[1] · **Amin Jalali**[1]

Received: 5 March 2018 / Accepted: 24 June 2018 / Published online: 28 June 2018

Abstract
The objective of this study is to compare the thermal stress changes in the tooth microstructures and the hydrodynamic changes of the dental fluid under hot and cold stimuli. The dimension of the microstructures of eleven cats' teeth was measured by scanning electron microscopy, and the changes in thermal stress during cold and hot stimulation were calculated by 3D fluid–structure interaction modeling. Evaluation of results, following data validation, indicated that the maximum velocities in cold and hot stimuli were -410.2 ± 17.6 and $+205.1 \pm 8.7$ μm/s, respectively. The corresponding data for maximum thermal stress were -20.27 ± 0.79 and $+10.13 \pm 0.24$ cmHg, respectively. The thermal stress caused by cold stimulus could influence almost 2.9 times faster than that caused by hot stimulus, and the durability of the thermal stress caused by hot stimulus was 71% greater than that by cold stimulus under similar conditions. The maximum stress was on the tip of the odontoblast, while the stress in lateral walls of the odontoblast and terminal fibril was very weak. There is hence a higher possibility of pain transmission with activation of stress-sensitive ion channels at the tip of the odontoblast. The maximum thermal stress resulted from the cold stimulus is double that produced by the hot stimulus. There is a higher possibility of pain transmission in the lateral walls of the odontoblast and terminal fibril by releasing mediators during the cold stimulation than the hot stimulation. These two reasons can be associated with a greater pain sensation due to intake of cold liquids.

Keywords Hydrodynamic theory · Odontoblastic transduction theory · Intensity of thermal stress · Fluid–structure interaction · Scanning electron microscopy

1 Introduction

Dentine is the location where the bioactive molecules have been accumulated. The cellular appendages of odontoblasts have extended into dentine and tubular structures called dentinal tubules. Dentinal fluid flows into the intertubular space and the space between tubule and odontoblast. Hot and cold thermal loadings on teeth following repeated intake of hot and cold foods or drinks throughout the day can lead to mechanical stress, structural deformation, and pain signaling in the teeth (Oskui et al. 2014). This may also result in immediate and/or permanent damages to the tooth tissues. Further, the thermal stress due to these thermal loadings may also lead to cracks accompanied by pain, damage or decreased longevity in teeth (Lin et al. 2010; Gholampour et al. 2016). Hence, dental thermal pain is an underlined issue and its addressing is of great importance.

The thermal pain in tooth is not similar to pain in other body parts, and its precise mechanism is ambiguous too (Lin et al. 2014). In general, three theories have been presented to explain dental thermal pain: neural theory, odontoblastic transduction theory and hydrodynamic theory. The neural theory states that noxious temperatures are directly transferred by dental primary afferent neurons (Chung et al. 2013; Lin et al. 2014). Odontoblastic transduction theory emphasizes the sensory role of odontoblasts in the thermal stimulation of tooth (Chung et al. 2013; Lee et al. 2017). Various studies have been conducted to prove the mentioned theories, and of course, some studies have questioned the validity of these two theories (Brännström 1986; Chung et al. 2013; Bleicher 2014). The hydrodynamic theory relates tooth pain to the movement of dentinal fluid inside tubule (Chung et al. 2013; Lin et al. 2014). Some other studies have concentrated on details of hydrodynamic theory in order to find out

✉ Seifollah Gholampour
s.gholampour@iau-tnb.ac.ir

[1] Department of Biomedical Engineering, Islamic Azad University-North Tehran Branch, P.O.B. 1651153311, Tehran, Iran

how dentinal fluid movement leads to pain transduction under thermal stimulation (Linsuwanont et al. 2007; Chung et al. 2013; Lin et al. 2014). Furthermore, various researches dealt with the type of receptors and ion channels and their role in dental pain-sensing (Hodgkin and Huxley 1952; Hille 1984; Caterina et al. 1997; Andrew and Matthews 2000; McKemy et al. 2002; Vongsavan and Matthews 2007; Lin et al. 2011b; Loyd et al. 2012; Chung and Oh 2013). There are, however, many controversies and ambiguities in these studies (Lin et al. 2014). In addition to the various mechanisms of the dental thermal pain transmission, many studies have pointed to the role of stress-sensitive ion channels in the thermal stimulation of teeth (Lin et al. 2011b, 2014). The thermal stress changes during cold and hot stimulations have been evaluated by some computer simulations (Oskui et al. 2013, 2014). However, the dentinal fluid and the tooth microstructures, including the dentinal microtubule, pulp, odontoblast and terminal fibril, were not considered in the thermal analysis of the previous simulations. Further, no comprehensive numerical computer simulation has been performed regarding the reasons of the greater pain caused by the cold stimulus than the hot stimulus.

From another point of view, the previous studies can be divided into two groups of human and animal studies. It should be noted that animal studies might be associated with problems or their results might be slightly different from those of human studies, and that the generalization of the results of animal studies to humans may be associated with some limitations. Pharmacologists have also confirmed that the prediction of human studies based on animal experience, especially for pharmaceuticals and environmental agents, may lead to poor prediction. The present animal study is not a molecular–cellular or physiological study of the dental thermal pain but calculates and compares the thermal stress changes in the tooth microstructures and the changes in hydrodynamic parameters of the dentinal fluid numerically under hot and cold stimuli in order to help to respond to the above ambiguities.

2 Materials and methods

2.1 Design of study

Some previous studies have done anatomical teeth investigation and examined tooth microstructures using scanning electron microscopy (SEM) (Lo Giudice et al. 2015; Cervino et al. 2017). In the present study, the dimensions of the tooth microstructures of eleven cat molars were measured by SEM using JEOL 2000 SEM (JEOL, Tokyo, Japan) (Fig. 1). It should be noted that according to the performed studies, the accuracy and detection limits of this device are adequate and sufficient for measurement of these dimensions (Trifkovic et al. 2012; Kuisma-Kursula 2017). First, the teeth crown was separated from the root and immediately after that a groove was made at the cementoenamel junction. The tool used for this purpose was a tungsten carbide bur which was cooled by water. More details of tooth preparation before scanning and the scanning protocol have been provided by a previous study (Garcés-Ortíz et al. 2015). After transferring the input data obtained from the SEM into the software Mimics v13.1 and producing the point clouds of the tooth components, the dimensions of the tooth microstructures were also calculated (Table 1). Subsequently, these point clouds were transferred to the CATIA R20 software. Then, a 3D model of seven sets of the molar microstructures including the dentinal microtubule, pulp, odontoblast, terminal fibril and dentinal fluid was created for each cat tooth in CATIA software (Fig. 2a, b). It should be noted that their number in each tooth is much greater than seven sets but only seven sets were modeled due to some limitations. Further, one terminal fibril was considered exactly for each set according to the study by Fearnhead (Fig. 2a, b) (Fearnhead 1957). Thereafter, these 3D mod-

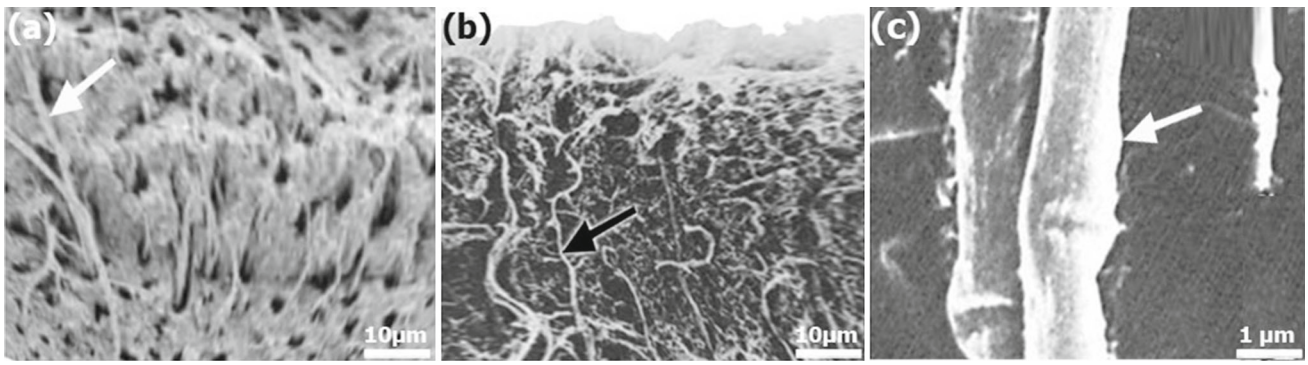

Fig. 1 Scanning electron microscopy image of cat tooth No. 1. **a** Tubule (white arrow), **b** dentino-enamel junction. Odontoblast (black arrow), **c** odontoblast (white arrow)

Table 1 Material properties and dimensions of tooth components

Properties	Tooth components	Value	References
Density (kg m^{-3})	Microtubule	1.96×10^{-3}	Lin et al. (2017)
	Terminal fibril	1.00×10^{-3}	Lin et al. (2017)
	Pulp	1.00×10^{-3}	Lin et al. (2017)
Elastic modulus (GPa)	Microtubule	20.00	Lin et al. (2017)
	Pulp	0.0021	Borčić et al. (2007)
	Odontoblast	3.18×10^{-7}	Metzger and Niebur (2016)
Poisson ratio	Microtubule	0.25	Lin et al. (2017)
	Pulp	0.45	Borčić et al. (2007)
	Odontoblast	0.48	Metzger and Niebur (2016)
Dynamic viscosity (kg/m s)	Dentinal fluid	1.55×10^{-3}	Lin et al. (2014)

Dimensions	Value
Inner diameter of tubule (μm)	0.75 ± 0.07
Maximum diameter of odontoblast (μm)	0.51 ± 0.05
Length of odontoblast (without cell body) (μm)	2.06 ± 0.16
Diameter of terminal fibril (μm)	0.07 ± 0.01
Length of terminal fibril (μm)	1.21 ± 0.11

els were transferred to ADINA 8.3 software (Adina R&D Inc., Watertown, MA, USA) for meshing and analysis. The 3D model of the microstructures of each tooth was analyzed under two thermal conditions of hot and cold stimuli to examine the changes of thermal stress due to the intake of hot and cold drinks and foods. Moreover, dentinal fluid circulation and its interaction with tubule, odontoblast and terminal fibril during hot and cold stimuli were also evaluated.

2.2 Computational analysis

The finite element method (FEM) has been the most common method for examining the dental pain mechanism caused by thermal stimulation in previous dental simulations (Oskui et al. 2013, 2014). However, only the solid phase can be analyzed in FEM and there is no possibility for defining and analyzing the fluid phase. Therefore, only the solid phase including the dentinal microtubule, pulp, odontoblast and terminal fibril can be analyzed while using this method for the thermal analysis and the fluid phase (dentinal fluid) is not examined. The analysis of the dental pain mechanism using FEM is hence incomplete and this method is not recommended.

Further, several studies have confirmed the deformation or probability of deformation in odontoblast, terminal fibril and tubule inner walls during thermal stimulation (Linsuwanont et al. 2008; Lin et al. 2011a, 2014). Therefore, tubule inner walls, walls of odontoblast and terminal fibril should be assumed as deformable boundaries for data analysis. On the other hand, one can only consider the effect of the fluid phase in problem-solving when the computational fluid dynamic (CFD) is used. The changes in the solid phase and the deformations of the walls between the fluid and solid phases cannot be applied in this method. The CFD method is hence not recommended for analysis of the dental thermal pain mechanism as this method is only able to analyze the dentinal fluid. Using the fluid–structure interaction (FSI) method, however, one can consider the simultaneous interaction of the solid (dentinal microtubule, pulp, odontoblast and terminal fibril) and fluid (dentinal fluid) phases. Thus, the FSI method in ADINA software was chosen for analysis of the pain in the present study so that it was possible to consider the deformation of boundaries and the effect of dentinal fluid. For analysis of solid and fluid phases, the arbitrary Lagrangian–Eulerian equations and the fully coupled FSI simulations were applied. The fluid–structure coupling was solved by an iterative solution based on full Newton–Raphson method. The procedure was iterated as long as the results reached the desirable convergence. Equation (1) is employed for formulating the fluid domain (Gholampour et al. 2017a; Gholampour 2018):

$$\rho_F \frac{\partial \boldsymbol{u_F}}{\partial t} + \rho_F((\boldsymbol{u_F} - \boldsymbol{W}).\nabla)\boldsymbol{u_F} = -\nabla p + \mu \nabla^2 \boldsymbol{u_F} + \boldsymbol{f_F^B} \tag{1}$$

where $\boldsymbol{W}$ is the velocity vector of the moving mesh; μ and p are the dynamic viscosity and pressure of dentinal fluid,

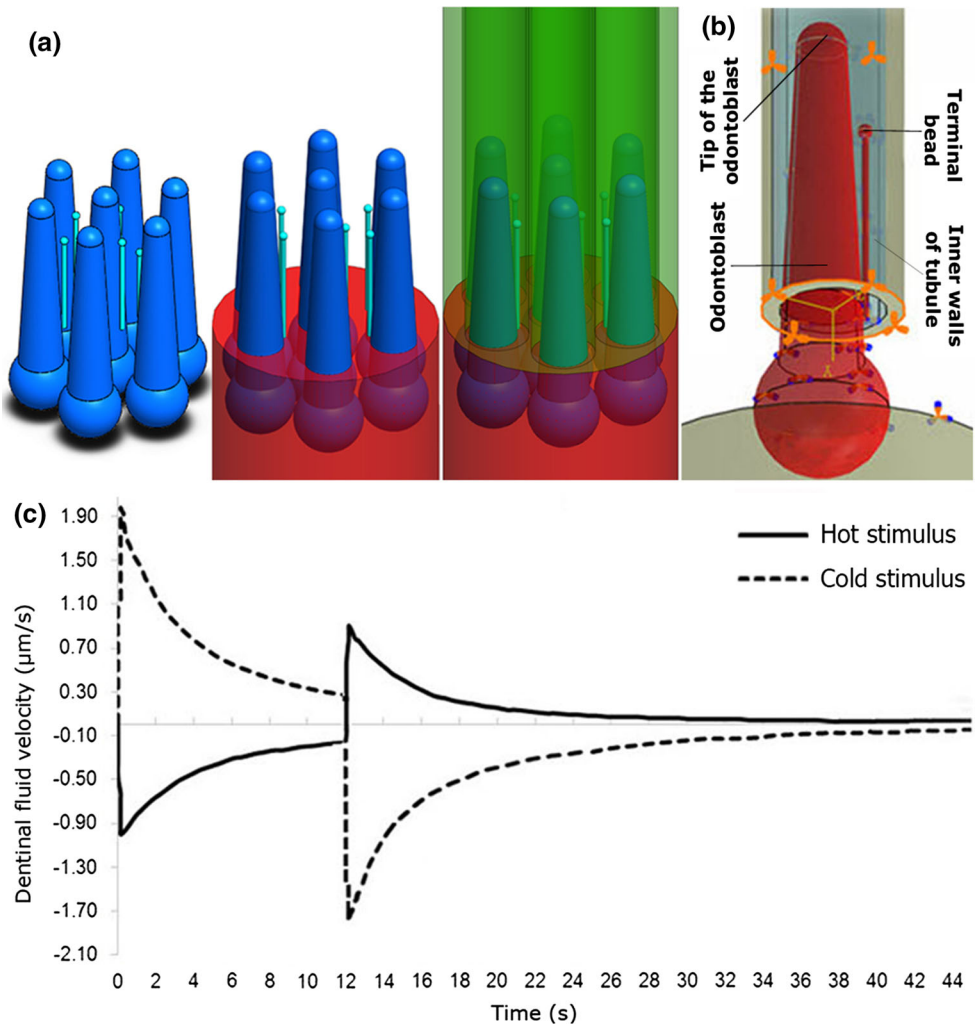

Fig. 2 **a** 3D model of dentinal microtubule, pulp, odontoblast and terminal fibril of cat tooth No. 1, **b** the red surfaces (odontoblast and terminal fibril) and the inner layer of tubule represent FSI boundaries, **c** the velocity diagram of the cold stimulus (dash) and the velocity diagram of hot stimulus (line). The cold stimulus diagram was obtained by applying a temperature of 5 °C and returning it to 37 °C, and the hot stimulus diagram was obtained by applying a temperature of 55 °C and returning it to 37 °C

respectively. ρ_F and $\boldsymbol{u_F}$ are density and velocity of dentinal fluid, respectively. $\boldsymbol{f_F^B}$ is the body force per unit volume, and $(\boldsymbol{u_F} - \boldsymbol{W})$ in ALE is the relative dentinal fluid velocity with respect to the moving coordinate velocity. Equation 2 governs the solid domain (Gholampour et al. 2017a; Gholampour 2018).

$$\nabla.\boldsymbol{\sigma_S} + \boldsymbol{f_F^B} = \rho_S \ddot{\boldsymbol{u}}_S \tag{2}$$

where $\ddot{\boldsymbol{u}}_S$ is the local acceleration of the solid model. ρ_S and $\boldsymbol{\sigma_S}$ are, respectively, the density and the stress tensor of the solid model. Dentinal fluid and solid domain were assumed as Newtonian fluid and linear elastic model, respectively. Table 1 presents the biomechanical characteristics of teeth components (Borčić et al. 2007; Lin et al. 2014, 2017; Metzger and Niebur 2016). It should be noted that the odontoblast is a soft tissue with material properties similar to those of enriched bone marrow cells (Huang 2009; Huo et al. 2010). Thus, the biomechanical properties of enriched bone marrow cells are considered for the odontoblast in Table 1.

2.3 Boundary conditions

For analysis, displacement and rotation in pulp and outer surfaces of tubules were fixed and constrained completely in three directions and all odontoblastic rotations and movements were completely constrained except along the longitudinal axis of tubule (Wang et al. 2015). The no-slip boundary conditions governed the non-deformable interfaces. The red surfaces (odontoblast and terminal fibril) and the inner layer of tubule in Fig. 2b represent deformable interfaces (FSI boundaries). The displacement equations and traction equilibrium for the FSI boundaries were similar to those in the literature (Gholampour et al. 2017b).

The results of previous studies also showed that the velocity vector of dentinal fluid has reverse directions in hot and cold stimuli (Horiuchi and Matthews 1973; Andrew and Matthews 2000; Lin et al. 2011a, b). Hence, the direction of dentinal fluid flow into the pulp in hot stimulus was considered to be opposite to that under cold stimulus. The main cause of the flow direction change during the hot and cold

stimulation is the expansion or contraction of the tubular fluid as well as the displacement of the walls of the tubule and odontoblast (Lin et al. 2014). So according to the results of previous studies, inlet and outlet flow and dentinal fluid velocity diagram (Fig. 2c) were considered in hot and cold stimulation (Matthews 1977; Charoenlarp et al. 2007; Lin et al. 2014).

2.4 Grid independence study

The study of grid independence was done as an essential part for making sure of having accurate solutions for numerical solutions. The step size was 1×10^{-5} s. The element type used for meshing all models except for the tubule was tetrahedral, and the element used for meshing the tubule was hexahedral. The numbers of the original elements in the odontoblast, microtubule and dentinal fluid of the animal No. 3 were 15,640, 43,410, and 123,870, respectively. Further, the differences of the maximum velocity of the dentinal fluid and stress between fine and medium meshes due to hot and cold stimuli in all eleven specimens were less than 0.07 and 0.09%, respectively (Fig. 3). The numerical simulations with smaller step sizes showed no significant difference. Therefore, the grid independence and convergence of results were ensured.

2.5 Velocity measurement

To ensure the correctness of the assumptions and software solution, the dentinal fluid velocity in the molars of eleven cats were measured experimentally using the method used in a recent study by Boreak et al. (2015) compared with FSI simulation results. It should be noted that producing the SEM images of tooth and in vitro tests to measure the experimental velocity of the dentinal fluid should be done on a completely healthy tooth without any prior damages. Since the extraction of a healthy human tooth was not allowed according to the ethical rules for approval of the studies of researches, the present study was done on eleven cat teeth.

To do this, the coronal dentine was cut from the pulp horn perpendicular to the vertical axis using a diamond wafer saw microtome. To remove the smear layer, the sample was cleaned with a 0.5 M EDTA solution (pH 7.4) for 2 min and rinsed with deionized water. The sample was then placed in a split chamber column, according to previous studies, for detecting the liquid flow and measuring the dentine permeability. The photochemical measurement was used in this regard (Ishihata et al. 2009, 2011). The chamber, which was on the occluded side of the sliced surface with a glass cover slip, was filled with a chemical illuminant reagent (aqueous solution of 0.02% luminol [5-amino-2,3-dihydro-1,4-phthalazinedione] and 1% sodium hydroxide), and the opposite chamber was filled with an activator solution (1% potassium ferricyanide and 1% hydrogen peroxide), which acted as a trigger for the chemiluminescence reaction. Following the creation of an external pressure, the trigger solution was injected into the pulp chamber. The solution then flowed through the dentine tubules into an occluded chamber, which contained the illuminant reagent. This led to the production of a luminescence reaction. The external pressure applied behind the trigger solution (pulpal pressure) in each specimen was regulated according to the values calculated from the FSI simulation results of pulpal pressure during hot and cold stimuli. For example, these values were assumed to be 8.5 and 17 cmHg for simulating the hot and cold stimuli in specimen No. 1, respectively.

Finally, the photosignal was registered with a photomultiplier tube detector (S10723, Hamamatsu Photonics, Hamamatsu, Japan). All equipment was placed in a light-proof container to avoid any light signal that may interfere with the luminescence signal. Following the injection of the trigger solution in four successive runs, the delay of chemiluminescence reaction was measured in order to determine the duration of the trigger solution transfer through the tubules. The chemiluminescence reaction occurred as the solution reached the opposite chamber, which contained the luminol solution. The delay time was the needed time for transfer of the trigger solution through the dentine tubules of the slice and its values were used for calculation of the velocity of flow. It should be noted that a negative control was used to ensure the correctness of the fluid velocity measurement.

2.6 Statistical analysis

Statistical parameters such as mean value, standard deviation (SD), coefficient of variation (standard deviation divided by the mean value) were calculated using SPSS version 20.

3 Results

The results were calculated in five cycles. Given that the results of cycles four and five were quite similar, the results of the fourth cycle are presented in this section. It should be noted that the results for all seven sets of models were similar.

3.1 Data validation

Data validation is one of the main concerns in computer simulation studies. The results showed that the experimentally measured velocities of dentinal fluid in cold and hot stimuli were 302.3 ± 18.2 and 151.4 ± 9.3 μm/s, respectively. The corresponding velocities calculated by FSI simulation in the same location were 351.4 ± 17.3 and 180.7 ± 8.4 μm/s, respectively, an error of almost 20%. It should be noted that various reasons may lead to difference of 20% between the

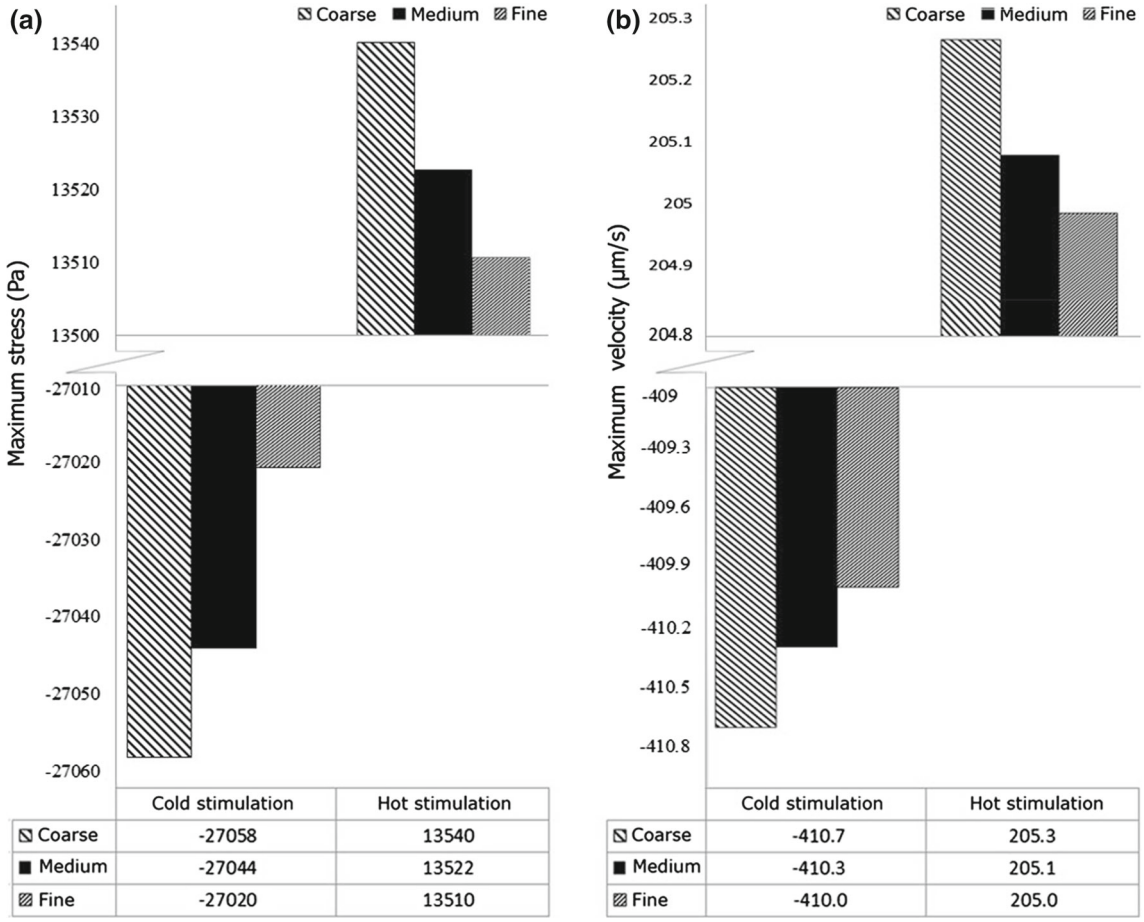

	Cold stimulation	Hot stimulation
Coarse	-27058	13540
Medium	-27044	13522
Fine	-27020	13510

	Cold stimulation	Hot stimulation
Coarse	-410.7	205.3
Medium	-410.3	205.1
Fine	-410.0	205.0

Fig. 3 **a**, **b** The three grid sizes (coarse, medium and fine) used in the grid independence study of cat tooth No. 3 for maximum stress and maximum dentinal fluid velocity under cold and hot stimuli, respectively

results. The results obtained from the experimental test for measuring the fluid velocity are largely dependent on the permeability of dentine (Horiuchi and Matthews 1973). Despite taking all considerations for choosing the tested fluid into account and considering a negative control in system, there is a considerable difference between the permeability of dentine in various individuals and even in different regions of the same tooth and this may be one of the reasons for the difference of 20% between experimental and simulation results. The important thing, however, is that in both experimental and FSI simulation results, the velocity value under cold stimulus was twice the value under hot simulation with an error of less than 3%. Thus, the simulation could reveal the main features of the dentinal fluid responses under thermal stimulation despite of the error.

Also, the results of pulpal pressure obtained from FSI simulation were also compared with the results of previous experimental studies. According to previous studies, pulpal pressure values in the absence of any thermal stimulation of teeth in a human, dog and cat were 1.04 ± 0.18, 2.41 ± 0.23 and 1.10 cmHg, respectively (Pashley et al. 1981; Vongsavan and Matthews 1992; Ciucchi et al. 1995). The method used in these studies has several errors and problems (Lin et al. 2011a). The corresponding pressure values calculated in the present study for hot and cold stimuli are 8.52 ± 0.20 and 17.07 ± 0.81 cmHg, respectively. Regarding the sample used in the study by Vongsavan and Matthews, it can be expressed that pulpal pressure due to hot and cold stimuli in the present study has increased about 8.2 and 16.3 times, respectively (Vongsavan and Matthews 1992). Due to the errors of the method applied by Vongsavan and Matthews, however, the values of 8.2 and 16.3 are not reliable, but this significant difference confirms the increase in pulpal pressure due to thermal stimulation.

Based on the reasonable conformity of FSI simulations and experimental velocities data of the dentinal fluid in the same cat tooth and also the comparison of pulpal pressure results, the validation of data was confirmed in this study. However, the experimental methods could not measure the distribution of dentinal fluid velocity or stress on the walls

of tubule, odontoblast and terminal fibril. These details were hence calculated using FSI simulation.

3.2 Evaluation of velocity, thermal stress and displacement

According to Table 2 and Fig. 4a, b, the maximum fluid velocities in cold and hot stimuli occurred exactly at the contact surface of dentinal fluid and the tip of the odontoblast and their values in cold and hot stimuli were -410.2 ± 17.6 and $+205.1 \pm 8.7$ μm/s, respectively, where the − and + signs indicate the direction of dentinal fluid flow toward tubule and toward pulp, respectively. Further, the maximum thermal stress caused by cold and hot stimuli equaled, respectively, to $-27{,}020.2 \pm 1053.2$ Pa (-20.27 ± 0.79 cmHg) and $+13{,}510.1 \pm 319.9$ Pa ($+10.13 \pm 0.24$ cmHg) and occurred in the tip of the odontoblast in both stimuli (Table 2, Fig. 4c, d). In addition, the – and + signs before the stress values indicate the compressive and tensile stresses. Moreover, compressive stress leads to contraction and tensile stress to expansion of tubule and odontoblast. The results also indicated that the maximum odontoblastic displacement in cold and hot stimuli was -1.26 ± 0.05 and $+0.63 \pm 0.03$ μm, respectively (Table 2, Fig. 4e, f), where – and + signs represent the direction of odontoblastic movement toward tubule and pulp, respectively. Finally, similar to the maximum velocity and thermal stress, the maximum displacement was higher under cold stimulus than hot stimulus. It should also be noted that the coefficient of variation for each parameter examined in eleven specimens was according to Table 2 less than 4.71% and in an acceptable range.

4 Discussion

4.1 Intensity and durability of thermal stress under hot and cold stimuli

First, the intensity of thermal stress was compared under hot and cold stimuli. The results indicated that cold stimuli led to contraction and decrease in the space between tubule and odontoblast, through which the dentinal fluid passes. The opposite happened with a hot stimulus. The maximum velocity of dentinal fluid under cold stimulus was two times that of hot stimulus (Fig. 5a). As the cross-sectional area of dentinal fluid flow pathway decreased in cold stimulus comparing to the hot stimulus, the velocity results were consistent with the law of continuity in fluid mechanics. According to Fig. 5a, the maximum thermal stress under cold stimulus was double that under hot stimulus. On the other hand, many studies have confirmed that the activation of stress-sensitive ion channels on nociceptors during thermal stimulation of teeth is one of the ways that can lead to transmission of pain signals (Lin et al. 2011a, 2014). The previous studies have also shown that the pain sensed during intake of cold drinks is greater than that during intake of hot drinks (Andrew and Matthews 2000; Lin et al. 2011b). Therefore, the numerical results of this study, which indicate that the intensity of thermal stress due to cold stimulus is twice that due to hot stimulus under similar conditions, can be associated with the greater pain due to cold stimulus than hot stimulus.

Figure 5b compares the thermal stress–time diagrams in both hot and cold stimuli in all eleven specimens. Based on these diagrams, the peak thermal stress due to hot and cold stimuli occurred after 1.36 ± 0.06 and 0.47 ± 0.02 s, respectively (Table 2, Fig. 5b). It means that cold stimulus affected the tooth almost 2.9 times faster than the hot stimulus. The thermal stress diagram in cold stimulus had a plateau shape and the stress reached almost to zero at 24.10 ± 0.94 s, whereas in hot stimulus this occurred at 41.00 ± 1.95 s (Table 2, Fig. 5b). This also means that durability of the thermal stress caused by hot stimulus was 71% more than that of cold stimulus. Therefore, the thermal stress caused by cold stimulus is much faster (2.9 times) but less durable (71%) than hot stimulus. As mentioned, the pain during the thermal stimulation of teeth can also be transmitted by activation of stress-sensitive ion channels. So considering these results and the + and − signs of stress values in hot and cold stimuli, it can be concluded that the function of ion channels may be so that their response to compressive stress (− sign for stress in cold stimulus) is faster but shorter, while their response to tensile stress (+ sign for stress in hot stimulus) is slower but more latent and durable.

4.2 Thermal stress in odontoblast under hot and cold stimuli

The purpose of this section is to compare the changes of thermal stress in the surfaces of odontoblast under hot and cold stimuli. The results obtained in Fig. 4a–d indicate that the odontoblast is the location of the maximum dentinal fluid velocity and stress following thermal stimulation. Odontoblasts generally mediate or modulate nociceptive transduction in dental nerve fibers (Shibukawa et al. 2015) and express thermosensitive transient receptors (Chung et al. 2013). Of course, the response of odontoblasts to thermal stimuli may not be necessarily entirely associated with nociceptive transmission to dental afferent nerve fibers terminated near odontoblasts, but considering that the thermal stress has reached to its maximum value on the tip of the odontoblast (Fig. 4c, d), it can be stated that under thermal stimulation, the tip of the odontoblast can transmit pain by activating stress-sensitive ion channels. On the other hand, the results indicate that the probability of activation of the stress-sensitive ion channels in lateral walls of odontoblasts and terminal fibrils is very low due to the low thermal stress in these areas

Table 2 The dentinal fluid velocities, thermal stresses, odontoblastic displacements, durability of the thermal stress and the time of the occurrence of the peak thermal stress in cold and hot stimuli

Specimen number	Maximum dentinal fluid velocity (μm/s)		Maximum thermal stresses (cmHg)		Maximum odontoblastic displacement (μm)		Durability of the thermal stress (s)		Time of the occurrence of the peak thermal stress (s)	
	Hot stimuli	Cold stimuli	Hot stimuli	Cold stimuli	Hot stimuli	Cold stimuli	Hot stimuli	Cold stimuli	Hot stimuli	Cold stimuli
1	+202.8	−409.5	+10.26	−19.34	+0.59	−1.33	42.11	25.15	1.28	0.46
2	+209.0	−397.3	+9.87	−20.10	+0.66	−1.28	38.05	24.85	1.42	0.47
3	+193.7	−382.2	+10.48	−20.42	+0.59	−1.18	40.35	23.64	1.29	0.45
4	+196.4	−405.5	+10.06	−21.33	+0.66	−1.27	44.04	25.05	1.36	0.47
5	+208.5	−427.8	+10.43	−19.55	+0.64	−1.19	39.08	24.38	1.45	0.51
6	+195.1	−396.6	+9.82	−20.18	+0.65	−1.27	43.08	24.25	1.34	0.48
7	+214.0	−426.0	+10.34	−21.10	+0.64	−1.31	40.15	25.27	1.44	0.51
8	+210.4	−419.0	+10.21	−21.77	+0.59	−1.26	43.35	23.19	1.39	0.45
9	+217.5	−421.4	+9.79	−19.70	+0.61	−1.19	41.54	24.26	1.37	0.46
10	+213.6	−436.1	+10.18	−20.34	+0.66	−1.22	42.85	22.37	1.35	0.47
11	+196.1	−388.6	+9.96	−19.51	+0.60	−1.34	39.15	24.26	1.27	0.45
Mean ± SD	+205.1 ± 8.7	−410.2 ± 17.6	+10.13 ± 0.24	−20.27 ± 0.79	+0.63 ± 0.03	−1.26 ± 0.05	41.00 ± 1.95	24.10 ± 0.94	1.36 ± 0.06	0.47 ± 0.02
Coefficient of variation (%)	4.20	4.31	2.42	3.90	4.70	4.50	4.71	3.92	4.54	4.60

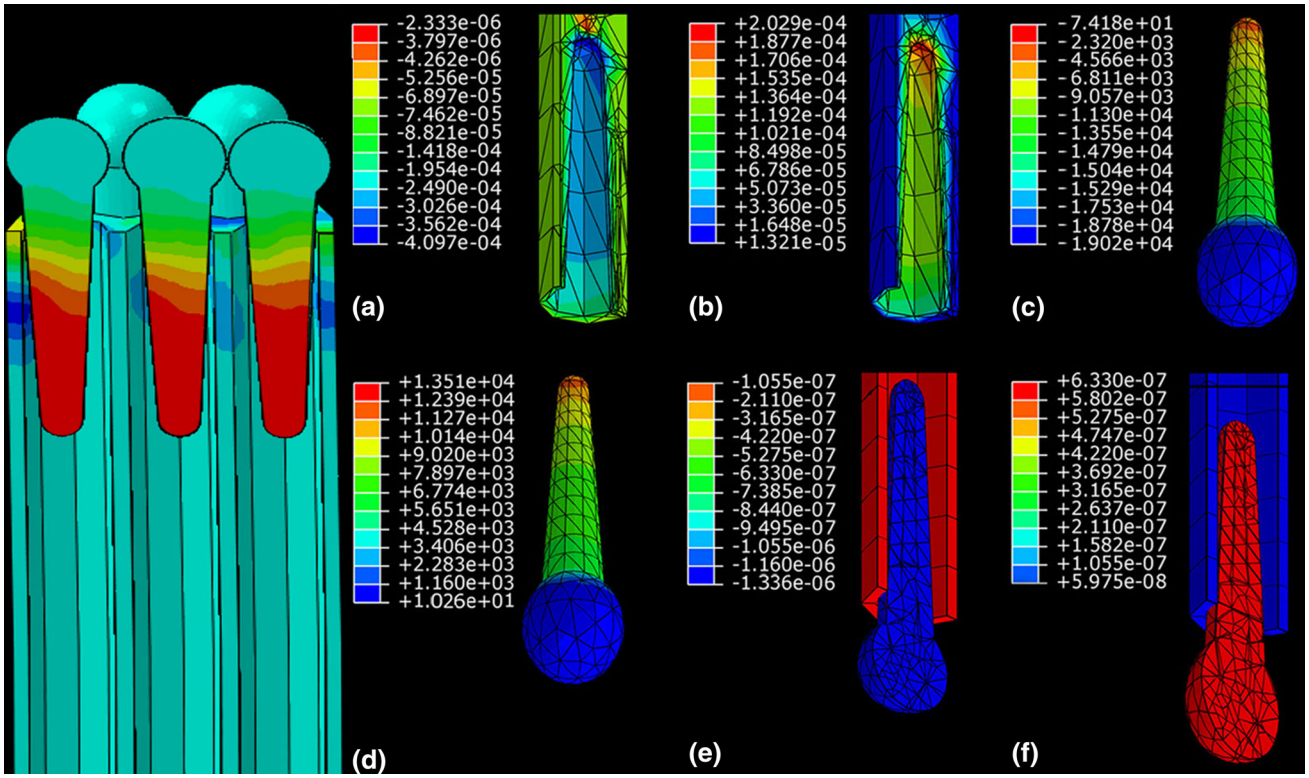

Fig. 4 **a**, **b** Velocity distribution (e^5 μm/s) under cold and hot stimuli, respectively, **c**, **d** the corresponding data for thermal stress (e^{-4} N $(\mu m)^{-2}$), **e**, **f** the corresponding data for displacement (μm). All panels belong to cat tooth No. 1

(Fig. 4c, d). However, it is possible that these two locations, considering the distances, can participate in the pain transmission mechanism by releasing mediators in the gap spaces (Loyd et al. 2012; Shibukawa et al. 2015; Khatibi Shahidi et al. 2015). That is the reason for examination of the gap spaces between lateral walls of odontoblast and terminal bead. Odontoblast gets away from terminal bead due to hot stimulus, whereas they get close to each other in cold stimulus (Fig. 4e, f). According to Fig. 5c-zoom M, for each 0.1 μm that the odontoblast moves toward the tubule under cold stimulus, the odontoblast comes circa 9 nm closer to terminal bead transversely. Thus, the decrease in gap space between odontoblast and terminal bead due to cold stimulus can lead to the higher possibility of pain transduction by lateral walls of odontoblast and terminal fibril through releasing mediators in this gap space under cold stimulus than hot stimulus. This result and that the intensity of thermal stress under cold stimulus is double the intensity of thermal stress under hot stimulus can be related to the higher pain sensation during intake of cold liquids than hot liquids. However, it should be generally considered that the mere evaluation of the role of odontoblast or stress-sensitive ion channels of odontoblast is not sufficient for thermal dental pain analysis because pain sensing is not deleted completely even after total removal of odontoblast according to a previous experimental study (Brännström 1986). The results of this section can be also useful in understanding the larger aspects of odontoblastic transduction theory.

4.3 Limitations and suggestions for future research

Since the branches of filaments could not be separated and measured in the SEM images, they were not considered in the modeling. It is also suggested that future studies perform a comprehensive molecular–cellular investigation of the tip and the lateral walls of odontoblasts in addition to thermal stress analysis. Finally, it is suggested that human studies similar to this study are conducted in the future to compare their results with the results of the present animal study and to make a definitive statement about dental thermal pain in human beings.

5 Conclusion

The thermal stress caused by a cold stimulus can influence much faster than hot stimulus, while the durability of the thermal stress caused by a hot stimulus is greater than that of cold stimulus. The decrease in the gap space between odontoblast and terminal bead due to cold stimulus can lead to the higher

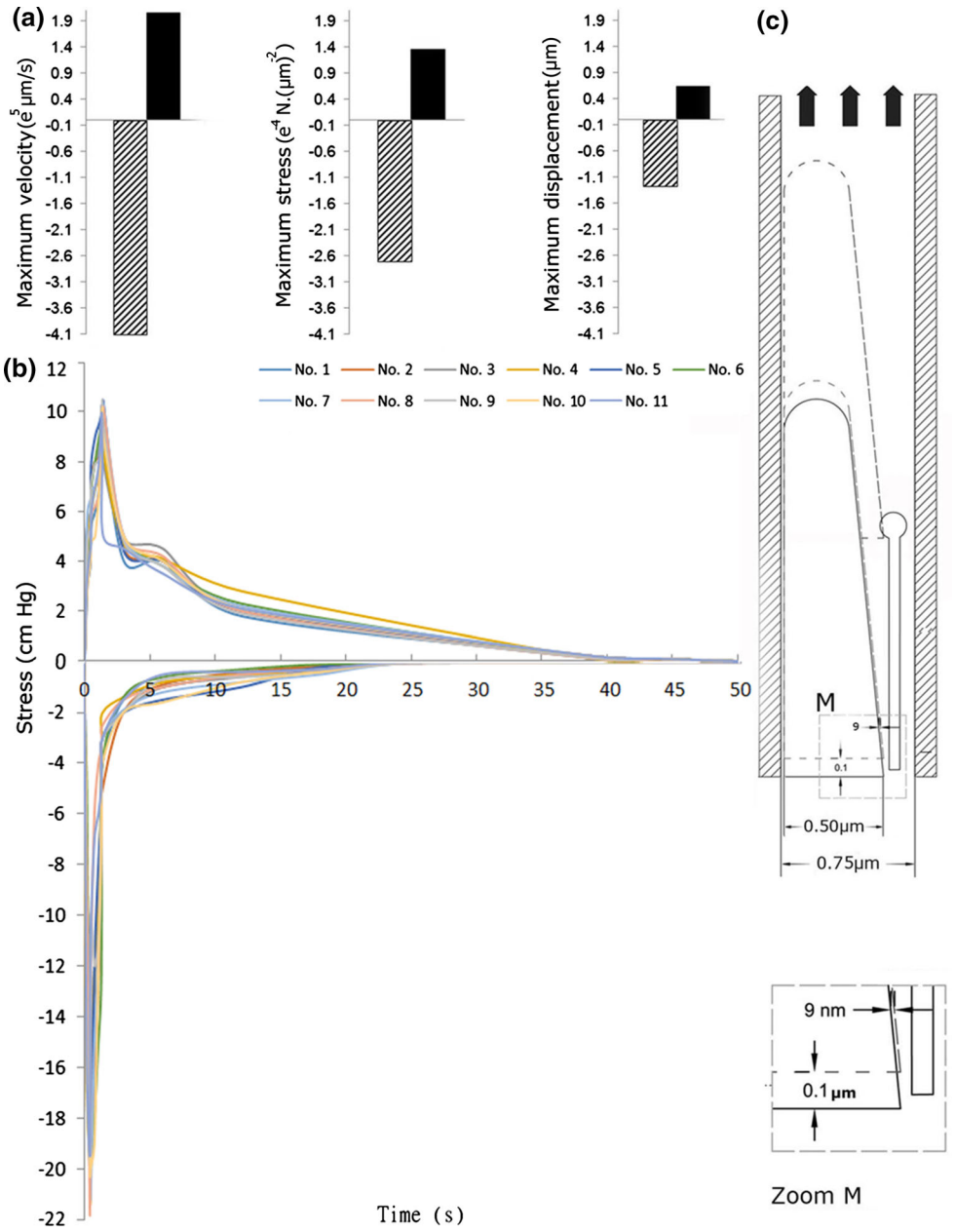

Fig. 5 **a** Comparison of maximum velocity, thermal stress and displacement under thermal stimulation. Solid and hatched areas show hot and cold stimuli, respectively. **b** Thermal stress–time diagrams were compared in thermal stimulation. The diagrams above and under the X-axis are related to the hot and cold stimulus in eleven cat teeth, respectively. **c** Odontoblast movement under cold stimulation

possibility of pain transduction by lateral walls of odontoblast and terminal fibril through releasing mediators in this gap space under cold stimulus than hot stimulus. This result and that the intensity of thermal stress under cold stimulus is twice the intensity of thermal stress under hot stimulus can be related to the higher pain sensation during intake of cold liquids than hot liquids.

Compliance with ethical standards

Conflict of interest All authors declare that they have no conflict of interest.

Ethical approval All procedures performed in studies involving human participants were in accordance with the ethical standards of Shohada Tajrish Hospital research committee North Tehran Branch, Islamic Azad University, Tehran, Iran (Ethics committee of biomedical research center) and with the 1964 Declaration of Helsinki and its later amendments or comparable ethical standards.

References

Andrew D, Matthews B (2000) Displacement of the contents of dentinal tubules and sensory transduction in intradental nerves of the cat. J Physiol 529:791–802

Bleicher F (2014) Odontoblast physiology. Exp Cell Res 325:65–71

Borčić J, Antonić R, Muhvić Urek M et al (2007) 3-D stress analysis in first maxillary premolar. Coll Antropol 31:1025–1029

Boreak N, Ishihata H, Shimauchi H (2015) A photochemical method for in vitro evaluation of fluid flow in human dentine. Arch Oral Biol 60:193–198

Brännström M (1986) The hydrodynamic theory of dentinal pain: sensation in preparations, caries, and the dentinal crack syndrome. J Endod 12:453–457

Caterina MJ, Schumacher MA, Tominaga M, Rosen TA, Levine JD, Julius D (1997) The capsaicin receptor: a heat-activated ion channel in the pain pathway. Nature 389:816–824

Cervino G, Fiorillo L, Spagnuolo G, Bramanti E, Laino L, Lauritano F, Cicciù M (2017) Interface between MTA and dental bonding agents: scanning electron microscope evaluation. J Int Soc Prev Community Dent 7:64

Charoenlarp P, Wanachantararak S, Vongsavan N, Matthews B (2007) Pain and the rate of dentinal fluid flow produced by hydrostatic pressure stimulation of exposed dentine in man. Arch Oral Biol 52:625–631

Chung G, Oh SB (2013) TRP channels in dental pain. Open Pain J 6:31–36

Chung G, Jung SJ, Oh SB (2013) Cellular and molecular mechanisms of dental nociception. J Dent Res 92:948–955

Ciucchi B, Bouillaguet S, Holz J, Pashley D (1995) Dentinal fluid dynamics in human teeth, in vivo. J Endod 21:191–194

Fearnhead RW (1957) Histological evidence for the innervation of human dentine. J Anat 91:267

Garcés-Ortíz M, Ledesma-Montes C, Reyes-Gasga J (2015) Scanning electron microscopic study on the fibrillar structures within dentinal tubules of human dentin. J Endod 41:1510–1514

Gholampour S (2018) FSI simulation of CSF hydrodynamic changes in a large population of non-communicating hydrocephalus patients during treatment process with regard to their clinical symptoms. PLoS ONE 13:e0196216

Gholampour S, Zoorazma G, Shakouri E (2016) Evaluating the effect of dental filling material and filling depth on the strength and deformation of filled teeth. J Dent Mater Tech 5:172–180

Gholampour S, Fatouraee N, Seddighi AS, Seddighi A (2017a) Evaluating the effect of hydrocephalus cause on the manner of changes in the effective parameters and clinical symptoms of the disease. J Clin Neurosci 35:50–55

Gholampour S, Fatouraee N, Seddighi AS, Seddighi A (2017b) Numerical simulation of cerebrospinal fluid hydrodynamics in the healing process of hydrocephalus patients. J Appl Mech Tech Phys 58:386–391

Hille B (1984) Ionic channels of excitable membrane. Sinauer Associates Inc, Sunderland

Hodgkin AL, Huxley AF (1952) A quantitative description of membrane current and its application to conduction and excitation in nerve. J Physiol 117:500–544

Horiuchi H, Matthews B (1973) In-vitro observations on fluid flow through human dentine caused by pain-producing stimuli. Arch Oral Biol 18:275–294

Huang GT (2009) Pulp and dentin tissue engineering and regeneration: current progress. Regen Med 4:697–707

Huo N, Tang L, Yang Z et al (2010) Differentiation of dermal multipotent cells into odontogenic lineage induced by embryonic and neonatal tooth germ cell-conditioned medium. Stem Cells Dev 19:93–104

Ishihata H, Kanehira M, Nagai T, Finger WJ, Shimauchi H, Komatsu M (2009) Effect of desensitizing agents on dentin permeability. Am J Dent 22:143–146

Ishihata H, Finger WJ, Kanehira M, Shimauchi H, Komatsu M (2011) In vitro dentin permeability after application of Gluma® desensitizer as aqueous solution or aqueous fumed silica dispersion. J Appl Oral Sci 19:147–153

Khatibi Shahidi M, Krivanek J, Kaukua N, Ernfors P, Hladik L, Kostal V, Masich S, Hampl A, Chubanov V, Gudermann T, Romanov RA (2015) Three-dimensional imaging reveals new compartments and structural adaptations in odontoblasts. J Dent Res 94:945–954

Kuisma-Kursula P (2017) Accuracy, precision and detection limits of SEM–WDS, SEM–EDS and PIXE in the multielemental analysis of medieval glass. X-Ray Spectrom 29:111–118

Lee BM, Jo H, Park G et al (2017) Extracellular ATP induces calcium signaling in odontoblasts. J Dent Res 96:200–207

Lin M, Xu F, Lu TJ, Bai BF (2010) A review of heat transfer in human tooth-experimental characterization and mathematical modeling. Dent Mater 26:501–513

Lin M, Liu S, Niu L, Xu F, Lu TJ (2011a) Analysis of thermal-induced dentinal fluid flow and its implications in dental thermal pain. Arch Oral Biol 56:846–854

Lin M, Luo ZY, Bai BF, Xu F, Lu TJ (2011b) Fluid mechanics in dentinal microtubules provides mechanistic insights into the difference between hot and cold dental pain. PLoS ONE 6:e18068

Lin M, Genin GM, Xu F, Lu T (2014) Thermal pain in teeth: electrophysiology governed by thermomechanics. Appl Mech Rev 66:030801

Lin M, Liu F, Liu S et al (2017) The race to the nociceptor: mechanical versus temperature effects in thermal pain of dental neurons. Acta Mech Sin 33:260–266

Linsuwanont P, Palamara JE, Messer HH (2007) An investigation of thermal stimulation in intact teeth. Arch Oral Biol 52:218–227

Linsuwanont P, Versluis A, Palamara JE, Messer HH (2008) Thermal stimulation causes tooth deformation: a possible alternative to the hydrodynamic theory? Arch Oral Biol 53:261–272

Lo Giudice G, Cutroneo G, Centofanti A, Artemisia A, Bramanti E, Militi A, Rizzo G, Favaloro A, Irrera A, Lo Giudice R, Cicciù M (2015) Dentin morphology of root canal surface: a quantitative evaluation based on a scanning electronic microscopy study. BioMed Res Int 27:ID164065

Loyd DR, Sun XX, Locke EE, Salas MM, Hargreaves KM (2012) Sex differences in serotonin enhancement of capsaicin-evoked calcitonin gene-related peptide release from human dental pulp. PAIN® 153:2061–2067

Matthews B (1977) Responses of intradental nerves to electrical and thermal stimulation of teeth in dogs. J Physiol 264:641–664

McKemy DD, Neuhausser WM, Julius D (2002) Identification of a cold receptor reveals a general role for TRP channels in thermosensation. Nature 416:52–58

Metzger TA, Niebur GL (2016) Comparison of solid and fluid constitutive models of bone marrow during trabecular bone compression. J Biomech 49:3596–3601

Oskui IZ, Ashtiani MN, Hashemi A, Jafarzadeh H (2013) Thermal analysis of the intact mandibular premolar: a finite element analysis. Int Endod J 46:841–846

Oskui IZ, Ashtiani MN, Hashemi A, Jafarzadeh H (2014) Effect of thermal stresses on the mechanism of tooth pain. J Endod 40:1835–1839

Pashley DH, Nelson R, Pashley EL (1981) In-vivo fluid movement across dentine in the dog. Arch Oral Biol 26:707–710

Shibukawa Y, Sato M, Kimura M, Sobhan U, Shimada M, Nishiyama A, Kawaguchi A, Soya M, Kuroda H, Katakura A, Ichinohe T (2015) Odontoblasts as sensory receptors: transient receptor potential channels, pannexin-1, and ionotropic ATP receptors mediate intercellular odontoblast-neuron signal transduction. Pflügers Arch Eur J Physiol 467:843–863

Trifkovic B, Budak I, Todorovic A, Hodolic J, Puskar T, Jevremovic D, Vukelic D (2012) Application of replica technique and SEM in accuracy measurement of ceramic crowns. Meas Sci Rev 12:90–97

Vongsavan N, Matthews B (1992) Fluid flow through cat dentine in vivo. Arch Oral Biol 37:175–185

Vongsavan N, Matthews B (2007) The relationship between the discharge of intradental nerves and the rate of fluid flow through dentine in the cat. Arch Oral Biol 52:640–647

Wang J, Jin X, Ma P (2014) Dentin–pulp tissue engineering and regeneration. In: Ma P (ed) Biomaterials and regenerative medicine. Cambridge University, Cambridge, pp 570-582